

Microstructure, mechanical properties and creep resistance of Mg–(8%–12%)Zn–(2%–6%)Al alloys

Xiao-feng WAN¹, Hong-jun NI¹, Ming-yu HUANG¹, Hua-li ZHANG¹, Jian-hua SUN²

1. School of Mechanical Engineering, Nantong University, Nantong 226019, China;

2. Department of Mechanical Engineering, Zilang College, Nantong 226019, China

Received 15 March 2012; accepted 25 December 2012

Abstract: The microstructural characteristics, mechanical properties and creep resistance of Mg–(8%–12%)Zn–(2%–6%)Al alloys were investigated to get a better overall understanding of these series alloys. The results indicate that the microstructure of the alloys ZA82, ZA102 and ZA122 with the mass ratio of Zn to Al of 4–6 is mainly composed of α -Mg matrix and two different morphologies of precipitates (block τ -Mg₃₂(Al, Zn)₄₉ and dense lamellar ε -Mg₅₁Zn₂₀), the alloys ZA84, ZA104 and ZA124 with the mass ratio of 2–3 contain α -Mg matrix and only block τ phases, and the alloys ZA86, ZA106 and ZA126 with the mass ratio of 1–2 consist of α -Mg matrix, block τ precipitates, lamellar ϕ -Al₂Mg₅Zn₂ eutectics and flocculent β -Mg₁₇Al₁₂ compounds. The alloys studied with the mass ratio of Zn to Al of 2–3 exhibit high creep resistance, and the alloy ZA124 with the continuous network of τ precipitating along grain boundaries shows the highest creep resistance.

Key words: Mg–Zn–Al alloys; microstructure; mechanical property; creep resistance

1 Introduction

Magnesium alloys are being increasingly used in the automobile industry in order to save mass thereby reducing fuel consumption and pollution. However, inferior mechanical properties of conventional Mg alloys at elevated temperatures limit the potential utilization of these alloys in important parts [1]. Among the various alloy systems developed, the commonly used magnesium alloys, such as AZ91 and AM60, are based on Mg–Al system, which have excellent castability, good room temperature mechanical properties and low cost. However, the use of these magnesium alloys has been limited to temperatures below 120 °C because of their poor heat resistance, especially creep property at elevated temperatures. The limitation is mainly due to the low melting point of the intermetallic phase Mg₁₇Al₁₂ in the microstructure, which is prone to softening at elevated temperatures [2,3]. Moreover, some magnesium alloys containing rare earth developed in the past few years have been found to possess higher heat resistance than conventional Al and Mg alloys [4]. However, the

alloys are extremely expensive, and pose a problem for mass production. Therefore, it is necessary to develop new heat-resistant magnesium alloys with low cost for elevated temperature applications. Recently, it was reported that alloys with high zinc and low aluminum (Mg–Zn–Al alloys) could meet the above requirements and would be an alternative to the presently used Mg–Al based alloys [5–8]. However, there is a lack of data concerning the microstructure of such alloys and information about the relationship between microstructure and mechanical properties, especially the effects of mass ratio of zinc to aluminum on creep resistance still remain unclear. From this point of view, a series of Mg–(8%–12%)Zn–(2%–6%)Al alloys were prepared and their microstructure and properties were investigated.

2 Experimental

Nine alloys whose compositions are listed in Table 1 were prepared in a mild steel crucible under the protection of mixed gas atmosphere of SF₆ (1%) and CO₂ (Bal.). Commercially pure Mg, Zn, Al and Mn (99%)

Table 1 Composition of experimental alloys (mass fraction, %)

| Alloy | Zn | Al | Mn | Mg |
|----------------------|-------|------|------|------|
| Mg–8Zn–2Al (ZA82) | 8.02 | 2.01 | 0.23 | Bal. |
| Mg–8Zn–4Al (ZA84) | – | – | – | – |
| Mg–8Zn–6Al (ZA86) | 8.11 | 6.12 | 0.25 | Bal. |
| Mg–10Zn–2Al (ZA102) | 9.87 | 1.95 | 0.27 | Bal. |
| Mg–10Zn–4Al (ZA104) | – | – | – | – |
| Mg–10Zn–6Al (ZA106) | 10.11 | 5.93 | 0.21 | Bal. |
| Mg–12Zn–2Al (ZA122) | 12.09 | 1.88 | 0.25 | Bal. |
| Mg–12Zn–4Al (ZA124) | 12.07 | 4.02 | 0.26 | Bal. |
| Mg–812Zn–6Al (ZA126) | 11.96 | 6.05 | 0.28 | Bal. |

stuffs were added to prepare these alloys. Mn was added to diminish the negative effect of the impurity Fe on corrosion resistance of the as-prepared alloy. The melt was held at 720 °C for several minutes before being poured into metal moulds made of cast steel. The compositions of the alloys prepared were measured by inductively coupled plasma atomic emission spectroscopy (ICP) and the results were well consistent with the designed compositions.

Tensile specimens with a gauge section of 18 mm×3.2 mm×1.8 mm were cut by electric spark machining from the ingots. The specimens selected at the corresponding position were homogenized at 335 °C by a SX-2.5-10 furnace. Creep specimens were machined according to the national standard GB2039—80 with dimensions of 10 mm in diameter and 100 mm in length and tested on a RD2-3 specified creep machine; the test temperature was monitored in three locations (top, middle and bottom) to maintain a temperature control of ±1 °C. Microstructure observations of the alloys were conducted on an Olympus optical microscope. The specimens were etched with a solution of 4% (mole fraction) nitric acid and ethyl alcohol for 5 s, and then flushed with ethyl alcohol. Further microstructural observations of the as-cast alloys as well as the micro-compositional analysis of phases were conducted on a Sirion FE scanning electron microscope (SEM) with the energy dispersive spectroscopy (EDS).

3 Results and discussion

3.1 Microstructure

The typical metallographs of several studied Mg–Zn–Al alloys are given in Fig. 1. It is found that the microstructure of these alloys consists of magnesium-rich α grains with the secondary phases distributed in interdendritic spacing along grain boundaries, and the distribution of the intermediate phases in the as-cast

microstructure shows different changing tendency with the various Al content or Zn/Al mass ratio.

The as-cast microstructures of the three alloys ZA82, ZA102 and ZA122 with the mass ratio of Zn to Al lying in 4–6 are shown in Figs. 1(a, b), from which two kinds of intermediate phases can be observed. One of them shows coarse block morphology (point A) and the other is a kind of dense lamellar eutectic structure (point B). The XRD patterns of the alloys ZA82 and ZA122 (Fig. 2(a)) indicate that these alloys are mainly composed of α -Mg and a small amount of $Mg_{32}(Al,Zn)_{49}$ phase named τ with a BCC structure (space group $Im\bar{3}$, $a=1.416$ nm [9]), and $Mg_{51}Zn_{20}$ phase, also known as ε , which has a BCT structure (space group $Immm$ with lattice parameter $a=1.4083$ nm, $b=1.4486$ nm, $c=1.4025$ nm [10]). Further detailed SEM observation reveals the morphology of these phases more clearly, as seen from Fig. 3(a). Micro-compositional analyses carried out by XEDS indicate that the elemental composition of block shaped precipitates and dense lamellar eutectic structure in ZA122 alloy corresponds to τ and ε phase, respectively. For the alloys, such as ZA84 and ZA104, with mass ratio lying in 2–3, some block lath shaped phases appear in the as-cast microstructure, as shown in Fig. 1(c). Furthermore, with the Zn content increasing, block precipitates observed in these alloys increase and become more continuous, as seen in the alloy ZA104 or ZA124 (Fig. 1(d)). On the basis of XRD patterns (Fig. 2(b)) and SEM analysis (Fig. 3(b)), the composition of the phase with block morphology is approximately equal to that of the τ phase mentioned above. Whereas with increasing Al content and correspondingly decreasing Zn/Al mass ratio, the block lath shaped phase present in the alloys ZA84, ZA104 and ZA124 reduces gradually in the three alloys containing 6% Al content, whose typical as-cast morphologies are manifested in Figs. 1(e,f), and OM micrographs taken from alloys ZA86 and ZA126, respectively, and exhibits a completely different microstructure characteristics. Under optical microscope, the microstructure of as-cast alloy ZA86 includes a small number of paralleled lamellar eutectics, which connect with some block precipitates distributed along dendritic boundaries in the form of a coarse continuously reticular structure, and additional compounds with flocculent morphology can also be observed near grain boundaries. Such feature becomes even more obvious in alloys ZA106 and ZA126. XRD patterns taken from the two alloys ZA86 and ZA126 are shown in Fig. 2(c), in which some peaks can be indexed as arising from the $\phi(Al_2Mg_5Zn_2)$ phase with an orthorhombic crystal structure (space group $Pbcm$, $a=0.90$ nm, $b=1.70$ nm, $c=1.97$ nm [11]) except for the remaining peaks of α -Mg

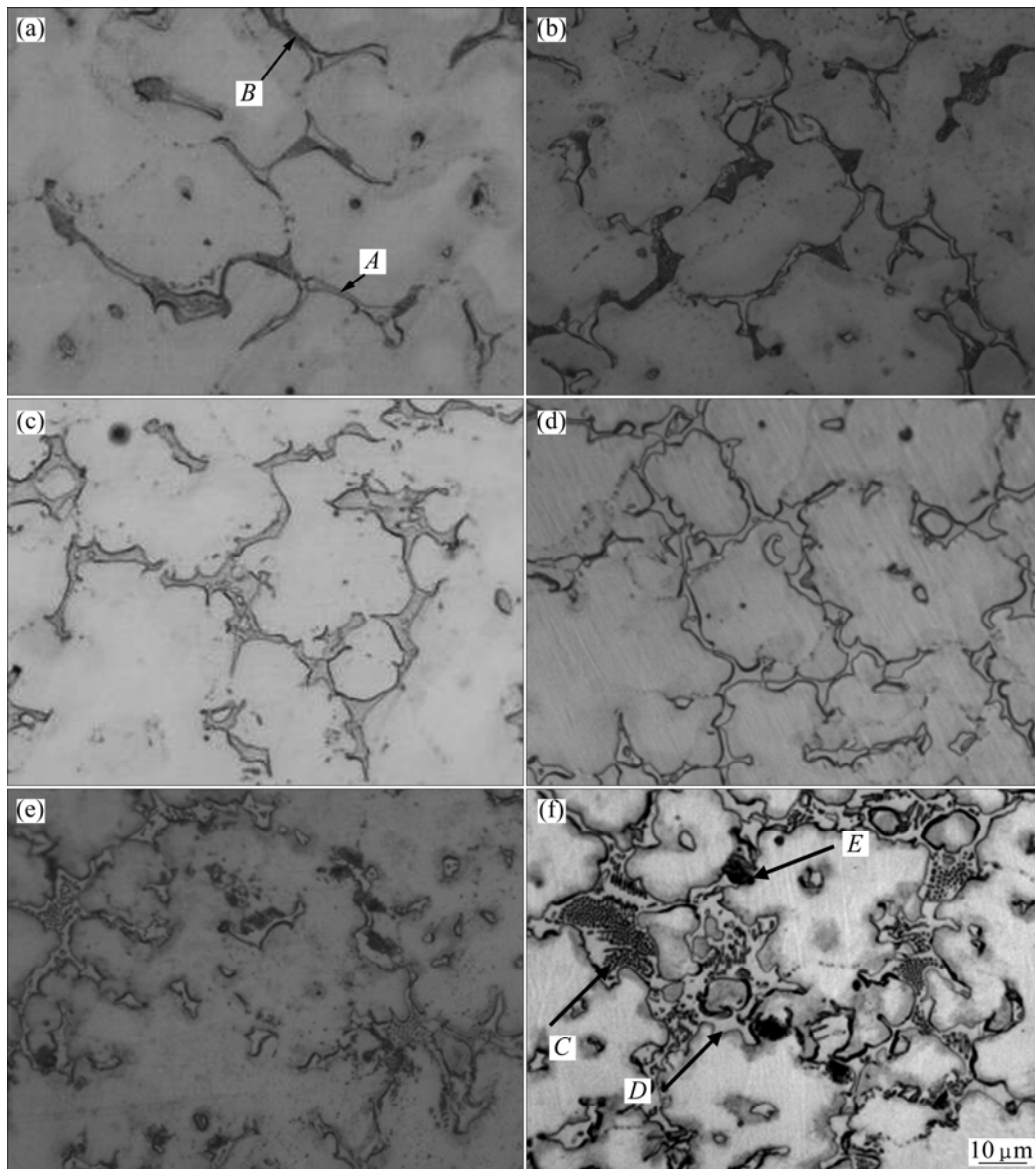


Fig. 1 Optical micrographs of as-cast alloys: (a) ZA82; (b) ZA122; (c) ZA84; (d) ZA124; (e) ZA86; (f) ZA126

matrix and τ phase. Figure 3(c) shows a typical SEM image of the as-cast alloy ZA126, which reveals relatively distinct microstructure. The result of microanalysis performed on the paralleled lamellar eutectic (point C) shows that the elemental composition of the lamellar precipitate corresponds to ϕ phase, and the block lath shaped phase (point D) is also validated as τ phase by XEDS analysis. Magnified flocculent morphology structure (point E) is illustrated in Fig. 3(d). It can be seen from the microanalysis that the flocculent compound is Mg- and Al-rich with a little amount of Zn contained and the mass ratio of Mg to Al is approximately close to that in the β ($Mg_{17}Al_{12}$) phase. In addition, the β phase could not be found in these alloys by X-ray diffraction which is attributed to low content and the limitation of test precision.

3.2 Mechanical properties

Tensile tests of the experimental alloys performed at elevated temperature of 175 °C are shown in Fig. 4. It can be seen that all the experimental alloys have similar high temperature strength for the exception of ZA82 and ZA84, with low element content, which have a relatively high ultimate strength. Additionally, high Zn and Al contents result in increasing yield strength but slightly decreasing elongation, such as ZA86, ZA124 and ZA126. It is probably because of the large amount of coarse intermetallics in the interdendritic spacing, which can hinder deformation and leads to the cutting effect on α -Mg matrix, thus resulting in the decline of mechanical properties. The results indicate that the type of precipitates in the alloys with different contents or Zn/Al mass ratio does not have any particular effect on

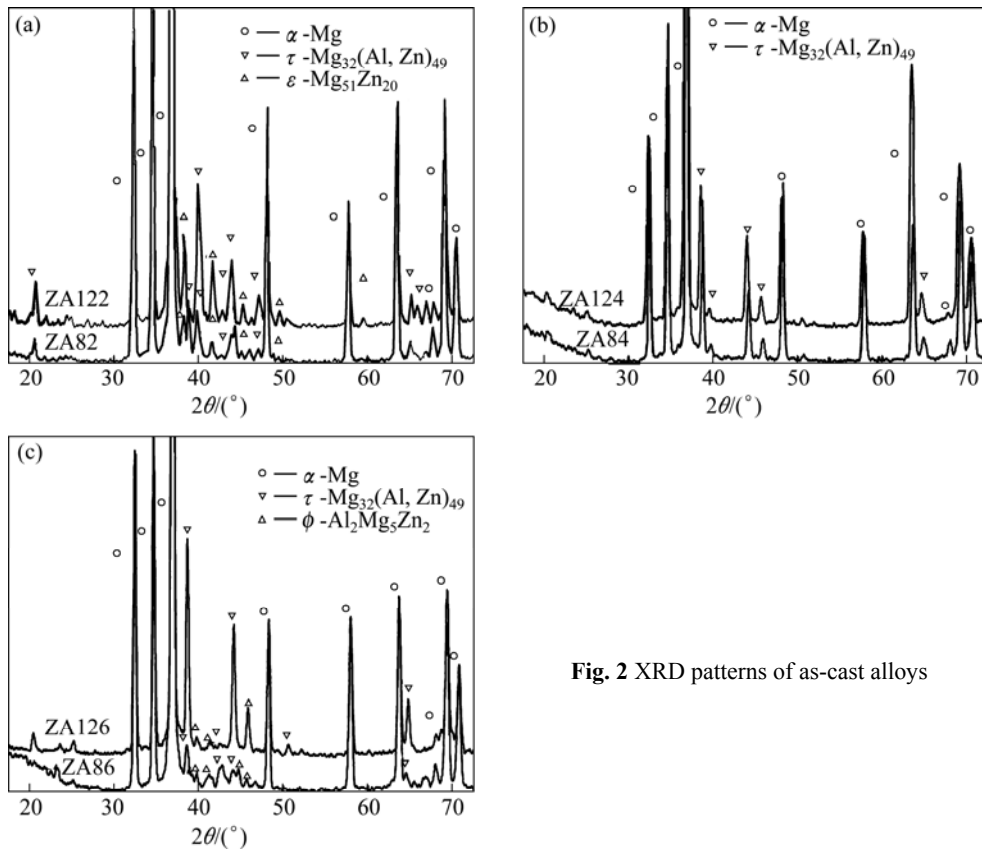


Fig. 2 XRD patterns of as-cast alloys

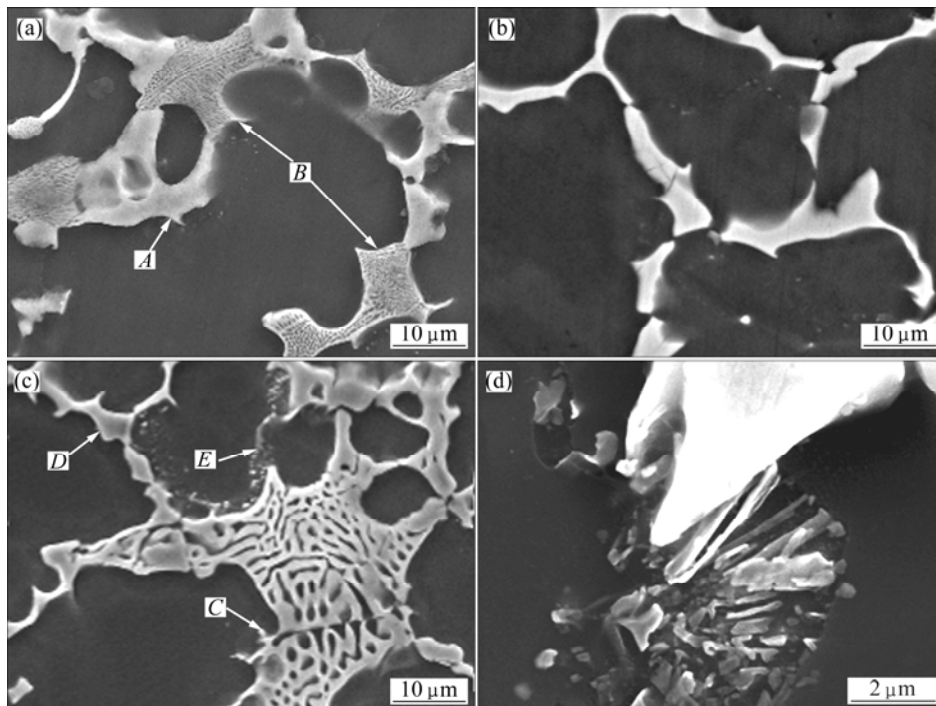


Fig. 3 SEM images of alloys: (a) ZA122; (b) ZA124; (c) ZA126; (d) Local magnification of point E in ZA126

the high temperature mechanical properties.

3.3 Creep properties

The creep curves obtained from as-cast alloys studied at 175 °C and 70 MPa are shown in Fig. 5. As

reference, the curves of AZ91 and AE42 in the same conditions are also shown, where the total creep extension measures the total time—dependent strain (creep strain). By measuring the slope of curves at steady stage, the minimum creep rate of the alloys can be

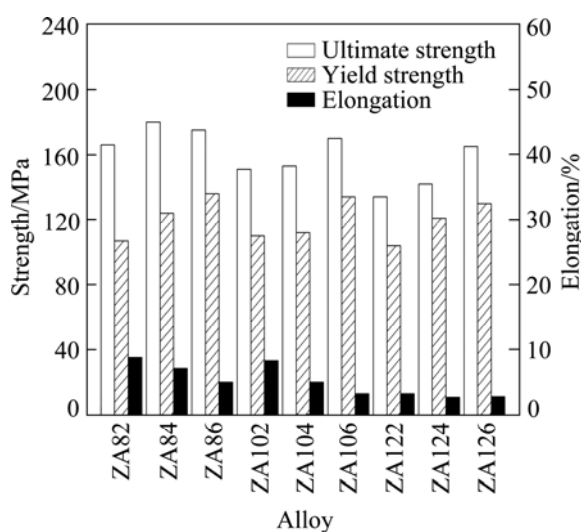


Fig. 4 Tensile properties of as-cast alloys studied at 175 °C

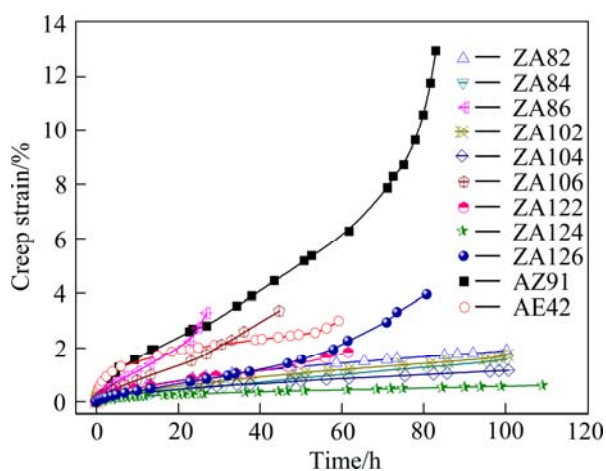


Fig. 5 Creep curves of alloys at 175 °C and 70 MPa

obtained. As seen from the figure, under the condition of 175 °C and 70 MPa, the steady slope and total creep strains of the experimental alloys exhibit the obvious difference with various element contents and Zn/Al mass ratios. The alloys ZA86, ZA106 and ZA126 with high Al content and low Zn/Al concentration ratio show lower creep life, rupturing after 27, 45 and 81 h, respectively, as well as higher creep rate and strains, and the alloy ZA122 also enters the accelerating creep stage with only 62 h creep life, indicating an inferior level in the creep resistance. Whereas, the creep resistances of alloys ZA84, ZA104 and ZA124 are comparable with those of alloys ZA82 and ZA102, maintaining lower steady creep rate and total strains under the same condition, and are far superior to AZ91, AE42, the conventional Mg–Al alloys.

The creep data of the alloys are summarized in Fig. 6, from which it can be seen that the lowest steady creep rate, obtained from alloy ZA124, is about $1.01 \times 10^{-8} \text{ s}^{-1}$, nearly one order of magnitude lower than that of the alloy AZ91, and the ZA124 alloy exhibits

lower creep strain as well as high creep life with better creep resistance. By comparison of alloy composition, it can be found that the creep resistance of alloys studied is related to the Zn/Al mass ratio, if the ratio is 2–3, the alloys exhibit high creep resistance, while the change of the Zn/Al mass ratio will lead to the decrease of the creep properties. Generally, the creep resistance of the alloys is notably independent of total element content.

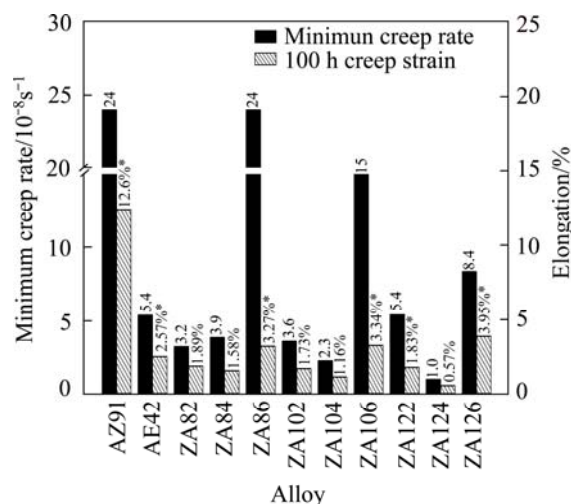


Fig. 6 Creep properties of alloys at 175 °C and 70 MPa (*—Elongation to fracture)

3.4 Analysis of creep properties

In order to understand the mechanism responsible for creep deformation of the alloys studied, SEM observations have been performed on the specimens after creep tests. In the specimen of the alloys Mg–(8%–12%) Zn–(2%–6%)Al after 100 h creep tests, different crack distributions are found on the secondary phases, as shown in Fig. 7. Figure 7(a) shows a SEM image taken from the specimen of alloy ZA82 after 100 h creep test. It can be seen that the morphology of the block lath shaped τ phase is almost the same with that in the as-cast microstructure, but few cracks appear on the dense lamellar eutectic ϵ phase. The specimen of alloy ZA122 shows more cracks on the lamellar eutectic structure with increasing crack spacing in comparison with ZA82 in the creep morphology (Fig. 7(b)). Figure 7(c) shows the microstructure of the specimen of the alloy ZA84 after creep test, which reveals relatively little cracks on the block τ phase. By comparison, in the alloy ZA124 the decreasing cracks on the continuous network τ phase exhibit more obviously, as shown in Fig. 7(d). In the specimens of alloys ZA86 and ZA126 after 100 h creep tests, the paralleled lamellar eutectic ϕ is distorted and the phase boundaries in the eutectic regions are not as clear as that as-cast microstructure before creep test. A great number of cracks can be observed on the block phases and lamellar eutectic structures, as shown in Figs. 7(e) and (f), respectively.

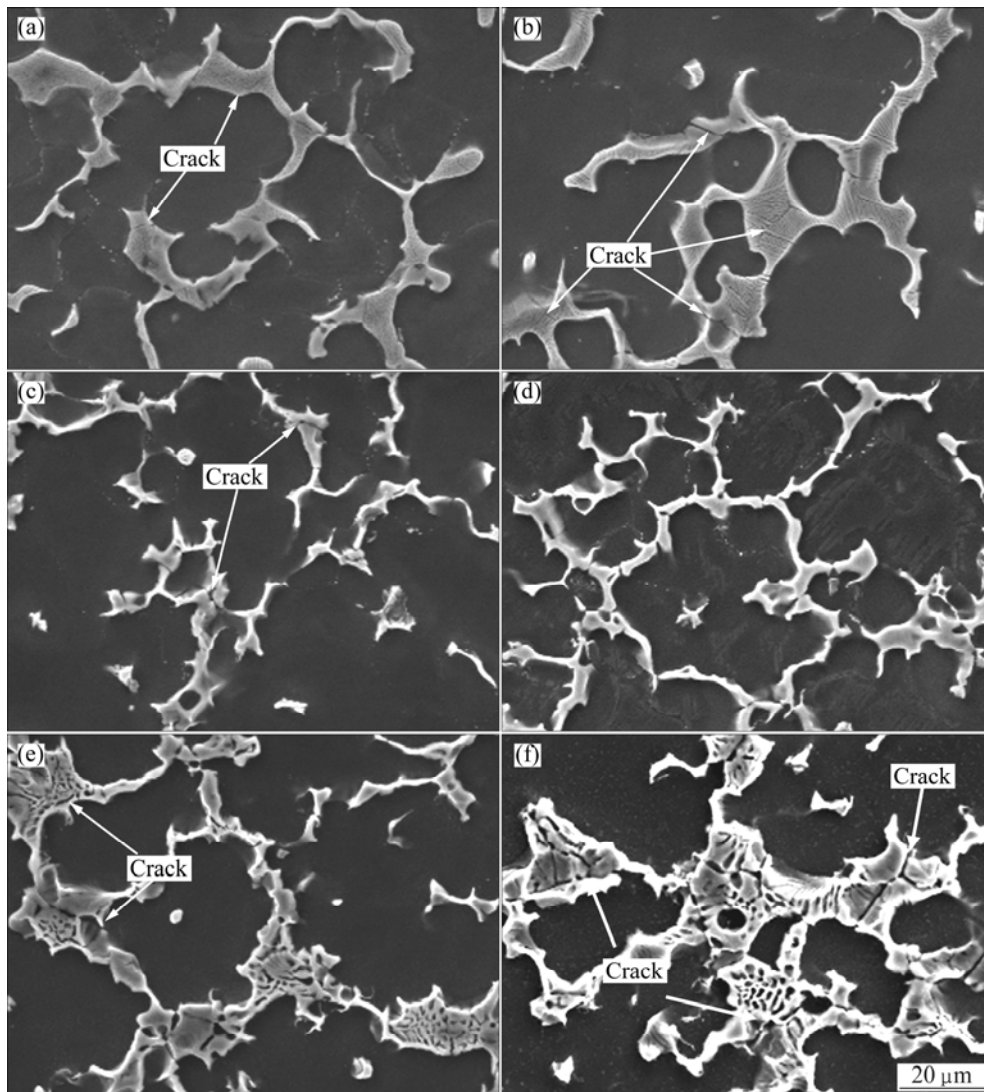


Fig. 7 SEM images of Mg–Zn–Al alloys after creep tests: (a) ZA82; (b) ZA122; (c) ZA84; (d) ZA124; (e) ZA86; (f) ZA126

According to the investigation mentioned above, the as-cast microstructures of Mg–Zn–Al alloys studied mainly consist of α -Mg, block shaped τ phase, dense lamellar ε phase, lamellar ϕ phase and flocculent β phase. The micro-structural parameters of these alloys, such as size, shape, distribution, and thermal stability, may exhibit different from each other. It is considered that thermal stability of mesophase, determined by melting and eutectic temperature, is a key factor that affects its capacity to improve creep resistance [8,12]. According to the Mg–Zn–Al ternary diagram [13,14], the τ phase has much high melting or eutectic temperature of 535 °C than the ϕ phase and ε phase, which melt at 393 °C and 341 °C, respectively. In the alloys with the mass ratio of Zn/Al ranging between 4 and 6, the dense lamellar ε phase and block shaped τ phase exist in the as-cast microstructure, and with increasing Zn content the volume fraction of low melting

point ε phase increases gradually. The creep resistance of alloy ZA122 exhibits an inferior level due to the large number of reticulate ε phase with a small amount of τ phase remaining at grain boundaries, which may be the channel of creep cracks initiation and propagation. Therefore, the alloy ZA122 with more Zn content shows lower creep property than that of alloy ZA82, which is consistent with the experimental data. For the alloys with the Zn/Al mass ratio between 2 and 3, the block τ phase with high thermal stability in the microstructure may play a positive role in improving creep resistance, especially in alloy ZA124, continuous network of τ precipitate at grain boundaries can effectively restrict neighboring grains relative motion along the grain-interface and improve the structural stability, thus may prevent the creep cracks during elevated temperature deformation and result in the high creep resistance. The inferior creep resistance of alloys with

the mass ratio between 1 and 2 is probably due to the small amount of lamellar ϕ eutectics connecting with block τ phase, compared with the τ phase, which has a much lower thermal stability and cannot effectively pin grain boundaries, leading to excess creep deformation by grain boundary sliding. Moreover, the creep properties of these high-aluminum content alloys may be affected by the low melting point of the intermetallic $\beta(\text{Mg}_{17}\text{Al}_{12})$ phase in these alloys, which is prone to softening at elevated temperatures, causing the grain boundary strength weaken significantly [15,16]. The appearance of the ϕ and β phases in as-cast microstructure of these alloys with low Zn/Al mass ratio indicates that increase of aluminum content and decrease of zinc content in the Mg–Zn–Al ternary alloys stabilize the two kinds of phases during non-equilibrium cooling. The result, obtained from microscopic observation, also reveals that the relative volume fraction of the ϕ and β phases in alloy ZA126 is slightly lower than that in alloy ZA86, which exhibits the highest creep deformation among the alloys studied.

4 Conclusions

1) The microstructures of the alloys ZA82, ZA102 and ZA122 with the mass ratio of Zn to Al ranging between 4 and 6 are mainly composed of α -Mg matrix and two different morphologies of precipitates (block $\tau\text{-Mg}_{32}(\text{Al}, \text{Zn})_{49}$ and dense lamellar $\varepsilon\text{-Mg}_{51}\text{Zn}_{20}$). The alloys ZA84, ZA104 and ZA124 with the ratio between 2 and 3 contain α -Mg matrix and only block τ phases. The alloys ZA86, ZA106 and ZA126 with the ratio between 1 and 2 consist of α -Mg matrix, block τ precipitates, lamellar $\phi\text{-Al}_2\text{Mg}_5\text{Zn}_2$ eutectics and flocculent $\beta\text{-Mg}_{17}\text{Al}_{12}$ compounds.

2) The type of precipitates in the alloys with different contents or mass ratio of Zn to Al does not have any particular effect on the high temperature tensile properties.

3) The alloys studied with the mass ratio of Zn to Al ranging between 2 and 3 exhibit high creep resistances, while the variation of the ratios leads to the decrease of creep properties.

4) The alloy ZA124 with the continuous network of τ precipitate at grain boundaries shows the highest creep resistance. The creep resistance of alloys decreases significantly due to ε eutectic phases, ϕ eutectics and β compounds appear, especially the creep properties of alloys containing ϕ eutectic phase and β phase with lower mass ration of Zn to Al are obviously inferior to other alloys.

References

- [1] SUZUKI A, SADDOCK N D, JONES J W, POLLOCK T M. Solidification paths and eutectic intermetallic phases in Mg–Al–Ca ternary alloys [J]. *Acta Materialia*, 2005, 53: 2823–2834.
- [2] LUO A A. Recent magnesium alloy development for elevated temperature applications [J]. *International Materials Reviews*, 2004, 49: 13–30.
- [3] PANTELAKIS S G, ALEXOPOULOS N D, CHAMOS A N. Mechanical performance evaluation of cast magnesium alloys for automotive and aeronautical applications [J]. *Journal of Engineering Materials and Technology*, 2007, 129: 422–431.
- [4] BETTLES C J, GIBSON M A, ZHU S M. Microstructure and mechanical behavior of an elevated temperature Mg-rare earth based alloy [J]. *Materials Science and Engineering A*, 2009, 505: 6–12.
- [5] ZHANG Chun-xiang, GUAN Shao-kang, LIU Tao, LI Shao-hua, LIU Zhong-xia. Effect of silicon on phase selection of ternary compounds during solidification of ZA84 magnesium alloy [J]. *Transactions of Nonferrous Metals Society of China*, 2011, 21(1): 52–57.
- [6] CHEN J H, CHEN Z H, YAN H G, ZHANG F Q, LIAO K. Effects of Sn addition on microstructure and mechanical properties of Mg–Zn–Al alloys [J]. *Journal of Alloys and Compounds*, 2008, 461: 209–215.
- [7] TARDIF S, TREMBLAY R, DUBÉ D. Influence of cerium on the microstructure and mechanical properties of ZA104 and ZA104 + 0.3Ca magnesium alloys [J]. *Materials Science and Engineering A*, 2010, 527: 7519–7529.
- [8] BALASUBRAMANI N, PILLAI U T S, PAI B C. Optimization of heat treatment parameters in ZA84 magnesium alloy [J]. *Journal of Alloys and Compounds*, 2008, 457: 118–123.
- [9] BERGMAN G, WAUGH J L T, PALLING L. The crystal structure of the metallic phase $\text{Mg}_{32}(\text{Al}, \text{Zn})_{49}$ [J]. *Acta Crystallographica*, 1957, 10: 254–259.
- [10] HIGASHI I, SHIOTANI N, UDA M, MIZOGUCHI T, KATO H. The crystal structure of $\text{Mg}_{51}\text{Zn}_{20}$ [J]. *Journal of Solid State Chemistry*, 1981, 36: 225–233.
- [11] BOURGEOIS L, MUDDLE B C, NIE J F. The crystal structure of the equilibrium ϕ phase in Mg–Zn–Al casting alloys [J]. *Acta Materialia*, 2001, 49: 2701–2711.
- [12] ZHANG J, GUO Z X, PAN F S, LI Z S, LUO X D. Effect of composition on the microstructure and mechanical properties of Mg–Zn–Al alloys [J]. *Materials Science and Engineering A*, 2007, 456: 43–51.
- [13] LIU Chu-ming, ZHU Xiu-rong, ZHOU Hai-tao. Magnesium phase diagram [M]. Changsha: Central South University of Technology Press, 2006: 154–159. (in Chinese)
- [14] REN Y P, QIN G W, PEI W L, LI S, GUO Y, ZHAO H D. Phase equilibria of Mg-rich corner in Mg–Zn–Al ternary system at 300 °C [J]. *Transactions of Nonferrous Metals Society of China*, 2012, 22(2): 241–245.
- [15] PARK K C, KIM B H, JO S M, KIM S H, PARK Y H, PARK I M. Mechanical and creep properties of the cast magnesium alloy [J]. *Applied Mechanics and Materials*, 2012, 152–154: 1207–1210.
- [16] PEKGULERYUZ M, CELIKIN M. Creep resistance in magnesium alloys [J]. *International Materials Reviews*, 2010, 55: 197–217.

Mg-(8%~12%)Zn-(2%~6%)Al 合金的组织、力学及高温蠕变性能

万晓峰¹, 倪红军¹, 黄明宇¹, 张华丽¹, 孙建华²

1. 南通大学 机械工程学院, 南通 226019;

2. 紫琅学院 机械工程系, 南通 226019

摘要: 研究了 Mg-(8%~12%) Zn-(2%~6%) Al 合金的微观组织特征、力学性能以及高温蠕变性能。结果表明, Zn/Al 质量比在 4~6 的 ZA82、ZA102 和 ZA122 合金的显微组织主要由 α -Mg、致密层片状 ϵ -Mg₅₁Zn₂₀ 相和块状 τ -Mg₃₂(Al, Zn)₄₉ 相组成。中等质量比(2~3)的 ZA84、ZA124 合金显微组织中的中间相主要为沿晶界呈半连续或连续分布的块状 τ 相。Zn/Al 质量比较小(1~2)的 ZA86、ZA126 合金显微组织中的中间相组织主要由块状 τ 相、层片状 ϕ -Al₂Mg₅Zn₂ 相和一些依附于这些中间相附近呈团絮状的 β -Mg₁₇Al₁₂ 相组成。Zn/Al 质量比值在 2~3 时, 合金的抗蠕变性能较好, 其中具有连续网状分布的块状 τ 相组织的 ZA124 合金显示出最好的蠕变抗力。

关键词: Mg-Zn-Al 合金; 微观组织; 力学性能; 蠕变性能

(Edited by Xiang-qun LI)